Article

Generating a sequence map of the pig pan-genome

Xiaomeng Tian[1*], Ran Li[1*], Weiwei Fu[1*], Yan Li[2*], Xihong Wang[1], Ming Li[1], Duo Du[1], Qianzi Tang[2], Yudong Cai[1], Yiming Long[1], Yue Zhao[1], Mingzhou Li[2#], Yu Jiang[1#]

[1]Key Laboratory of Animal Genetics, Breeding and Reproduction of Shaanxi Province, College of Animal Science and Technology, Northwest A&F University, Yangling 712100, China.

[2]College of Animal Science and Technology, Sichuan Agricultural University, Chengdu 611130, China.

[*]These authors contributed equally to this work.

[#]Corresponding author. E-mail: yu.jiang@nwafu.edu.cn (Y.J.) and mingzhou.li@sicau.edu.cn (M.L.).

Abstract

Pigs (*Sus scrofa*) exhibit diverse phenotypes in different breeds shaped by the combined effects of virous local adaptation and artificial selection. To comprehensively characterize the genetic diversity of pigs, we constructed a pig pan-genome by comparing 11 representative pig breeds of genome assemblies with the reference genome. Approximately 72.5 Mb non-redundant sequences were identified as "pan-sequences". On average, 41.7 kb of spurious heterozygous SNPs per individual were removed and 12.9 kb novel SNPs per individual were recovered using pan-genome, thereby providing enhanced resolution for genetic diversity of different pig populations. Analysis using Hi-C, RNA-seq data and homolog annotation indicates that these pan-sequences contain protein-coding exons and regulatory elements. Our supplied pan-sequences can further improve the interpretation of local 3D genomes. This pan-genome as well as the accompanied web-based repository will serve as a primary resource for genetic diversity exploration to promote agricultural production and biomedical research.

Introduction

Sus scrofa (i.e., pig or swine) is of enormous agricultural significance and an attractive biomedical model. Pigs were domesticated from wild boars independently in Anatolia and East Asia approximately 10,000 years ago following long-term gene flow from their local wild counterparts(Larson, et al. 2005; Groenen, et al. 2012; Frantz, et al. 2015). From domestication to modern breeding practices, the combined effects of local adaptation and human-driven artificial selection have shaped the genomes of domestic pigs. Genetic differences between diverse pig breeds underlie these extensive phenotypic variations, and to date, these variations have been interpreted largely in the context of the annotated reference genome by sequencing individual genomes and comparing reads to the reference. Guided by the most contiguous reference genome of the European domestic Duroc pig (the last assembly of Sscrofa11.1 is 2.50 Gb in length, with gaps of 29.86 Mb and 592 unplaced

scaffolds of 66.6 Mb) **(Supplementary Fig. 1)**, considerable effort has been devoted to unravelling the genetic control of phenotypes by sequencing individual genomes and comparing reads to the reference. Nonetheless, resequencing is limited in terms of capturing genetic variations and assessing variations in 'missing pieces' (i.e., gap or mis-assigned regions) of the reference genome. Alternatively, comparisons of independently *de novo*-assembled genomes and a reference genome sequence promise a more accurate and comprehensive understanding of genetic variation within a species(Li, et al. 2014).

Most recently, the pan-genome, the non-redundant collection of all genomic sequences of a species, has emerged as a fundamental resource for unlocking natural diversity in eukaryotes. Intraspecific comparisons in plants (e.g., soybean(Li, et al. 2014), Brassica oleracea(Golicz, et al. 2016), Brachypodium distachyon(Gordon, et al. 2017) and rice(Zhao, et al. 2018)) and in animals (e.g., mosquitoes(Neafsey, et al. 2015), macaques(Yan, et al. 2011) and humans(Li, et al. 2010; Maretty, et al. 2017)) have revealed surprisingly large amounts of variation within a single genome. To build a high-quality pan-genome, a number of individual genomes are required(Li, et al. 2014; Monat, et al. 2017; Wong, et al. 2018); which remains an obstacle for most mammalian species. Our previous studies generated *de novo* assemblies of ten geographically and phenotypically representative individual pig genomes from Eurasia with contig N50 from 57 kb to 102 kb(Li, et al. 2013; Li, et al. 2017). Together with a previously assembled genome of one Chinese Wuzhishan boar with a contig N50 size of 32 kb(Fang, et al. 2012), the availability of 11 individual pig genomes has provided an unprecedented opportunity to investigate detailed genetic differences at the individual, ethnic/breed or continental level.

To construct the pig pan-genome, we carry out an in-depth comparison between 11 *de novo* assemblies and the reference genome using an assembly-versus-assembly approach. Furthermore, we depict the three-dimensional (3D) spatial structure of the pan-genome using Hi-C data and reveal the characteristics of pan-sequences in A/B compartment (generally euchromatic and heterochromatic regions) and TAD levels.

We also build a publicly available database (PIGPAN, http://animal.nwsuaf.edu.cn/code/index.php/panPig) combined all these analysis results for the swine community, which will serve as a fundamental resource for unlocking variations within diverse pig breeds.

Results

Initial characterization of pan-sequences in the pig genome

To construct the pig pan-genome, we first aligned 11 assemblies from 11 diverse breeds (five from Europe, and six from China) against Sscrofa11.1 using BLASTN to collect the unaligned sequences **(Fig. 1a and Supplementary Fig. 2)**. The sizes of the unaligned sequences in the Chinese pigs were clearly larger than those in the European pigs **(Fig. 1a)**. As expected, the Wuzhishan assembly had the highest number of sequences because this sample is the only male individual among all the 11 assemblies and can provide many Y chromosome-linked sequences. **(Fig. 1a and Supplementary Table 2)**. After removing redundant sequences, we obtained 39,744 sequences with a total size of 72.5 Mb **(Fig. 1b)**, these sequences were absent from the reference genome and were thus defined as pan-sequences. The proportion of repetitive elements in these sequences (45.91%) were slightly higher than that of Sscrofa11.1 **(Fig. 1a)**. Additionally, the GC level (44.61%) was higher than that of Sscrofa11.1 (41.5%) **(Supplementary Table 3).** We further identified 44% of the pan-sequences as being specific to a single assembly, highlighting the limitations of using single assemblies **(Fig. 1b)**. Most of the pan-sequences were relatively short ranging from 300 bp to 5 kb. Nonetheless, 57.87% of the pan-sequence bases originated from sequences that are over 5 kb in length **(Fig. 1c)**.

To validate the authenticity of the pan-sequences, we first compared these sequences to ten mammalian genomes and found that the majority (67.5%) of the pan-sequences had homologs in these genomes (E-value < 1e-5) **(Fig. 2a and Supplementary Table 4)**. The number of best hits between the pan-sequences and the ten mammalian genomes were consistent with their evolutionary relationships with most best hits identified in Cetacea **(Fig. 2a)**. To explore the potential presence or

absence of protein-coding genes within the pan-sequences, we aligned the pan-sequences to Refseq proteins from pig, cattle, goat, human, sheep and sperm whale using TBLASTN (e-value < 1e-5). The most significantly abundant hits were members of the olfactory receptor family (12.4%), which is the largest gene superfamily in vertebrates(Zhang and Firestein 2002; Nguyen, et al. 2012) followed by other highly variable families (typically, O-methyltransferase domain-containing proteins) **(Fig. 2b)**. Especially, 18 new and complete olfactory receptor genes were identified (**Supplementary Fig. 3**), implying that our pan-sequences can ensure an enriched repertoire of highly divergent gene families.

To explore whether the presence or absence of pan-sequences exhibited population-specific characteristics, we retrieved 87 publicly available pig genomes and aligned them to all pan-sequences. The presence of each sequence in 87 individuals from China and Europe was determined by calculating their normalized read depth (NRD). Based on the presence of pan-sequences in the populations, all individuals were clustered into three distinct groups corresponding to their geographical distribution, including southern Chinese, northern Chinese and European pigs (> 10× coverage depth) (**Fig. 2c and Supplementary Table 5**), consist with the previously reported genetic architecture of domestic pigs(Ai, et al. 2015).

Furthermore, of the 87 pig genomes, 42 represented males, enabling us to determine whether the pan-sequences belonged to Y chromosome-linked sequences **(Supplementary Table 5)**. We identified 10.43 Mb of putative Y chromosome-linked sequences that were present in more than 90% of male individuals but absent in females **(Supplementary Table 6)**. The distribution pattern of these Y chromosome-linked pan-sequences revealed an Asian haplogroup which is confined to Asia and a Eurasian haplogroup which is distributed across Eurasia. This finding is concordant with previous reports(Guirao-Rico, et al. 2018), thus showing that we found a substantial number of novel Y chromosome-linked sequences that are absent in the present reference genome **(Fig. 2d)**.

To determine the potential genomic positions of the pan-sequences, we aligned

the pan-sequences to Sscrofa11.1 using their flanking sequences. Only 19.00% (7,554) of the pan-sequences could be anchored in this way **(Supplementary Table 7)**. By providing pan-sequences with refined positions, the genomic annotation could be enriched and improved. A pan-sequence of 14.3 kb containing the complete genic region of *RARRES3* was revealed and validated by resequencing and expression data (**Fig. 2e**). *RARRES3* acts as a tumour suppressor or growth regulator(Shyu, et al. 2003). Another pan-sequence of 18.6 kb included six coding exons of ZNF622 that are missing in Sscrofa11.1 (**Fig. 2e**). *ZNF622* played a role in embryonic development by activating the DNA-bound *MYBL2* transcription factor(Arumemi, et al. 2013). Based on whole-genome resequencing data, this sequence showed presence/absence variations, which in turn resulted in alternative splicing variants, as evidenced by the RNA-seq data.

Constructing a more comprehensive sequence map for genomic and transcriptomic analysis

Compared with Sscrofa11.1, the genomic mapping ratio of the six samples we chose was increased by 0.29-0.43% in the pan-genome **(Fig. 3a and Supplementary Table 8)**. In contrast, the mapping ratio of Sscrofa11.1 in the pan-genome was decreased by approximately 1.43%, indicating that many reads had been adjusted to better positions in the pan-sequences **(Fig. 3a)**. The adjustment of many reads from Sscrofa11.1 to pan-sequences will result in better SNP calling efficacy. An average of 41,729 heterozygous SNPs per sample were depressed **(Supplementary Table 9)**. Furthermore, 12,888 novel SNPs per individual were recovered using the pan-genome. The average read-mapping quality was significantly increased, and the read depth was also adjusted to the whole-genome average in the regions where spurious SNPs were removed **(Fig. 3b, c, d and Supplementary Fig. 4)**.

In addition, the transcriptomic mapping quality and mapping rate were also improved based on the RNA-seq data of 92 samples (**Supplementary Figs. 5 and 6**). In total, 897 sequences containing exonic regions showed appreciable expression (FPKM ≥ 1 in at least one sample). To further assess the protein-coding potential of

146 pan-sequences, a total of 607 out of the 897 pan-sequences were predicted to have
147 coding potential by Coding Potential Calculator (CPC)(Kong, et al. 2007). For the
148 gene expression of pan-sequences, more expression differences were found among
149 tissues (Pearson's r = 0.84) than within tissues (Pearson's r = 0.91), consistent with
150 previous findings(Tang, et al. 2017) **(Fig. 3e and Supplementary Fig. 7)**.

151 **Hi-C based analysis revealing the characteristics of pan-sequences regarding 3D**
152 **structures and their potential function**

153 Adjacent loci generally demonstrated frequent interaction as determined by the
154 high-throughput Hi-C analysis(Dong, et al. 2017); this enabled us to anchor the
155 pan-sequences to Sscrofa11.1 based on the mutual interactions. Here, we generated 12
156 Hi-C data from 10 individuals to anchor the pan-sequences to Sscrofa11.1 by inferring
157 their special interactions with adjacent regions **(Supplementary Tables 10 and 11)**.

158 To evaluate the robustness and accuracy of Hi-C based localization, we
159 comprehensively investigated the anchored results from five liver Hi-C samples
160 digested by the MboI enzyme and another seven samples digested with HindIII
161 enzyme (see methods). The result indicates that the Hi-C-based localization has high
162 consistency and higher sequencing coverage could lead to higher localization rate
163 **(Supplementary Fig. 8 and 9)**. A total of 7,554 sequences (19.0%) can be anchored
164 to Sscrofa11.1 by flanking sequences. Using Hi-C based approach, another 3447
165 sequences can be further anchored. Based on this result, at 100-kb resolution, we
166 found the pan-sequences are uniformly distributed in A/B compartment which are
167 generally euchromatic and heterochromatic regions, respectively(Dogan and Liu 2018)
168 **(Fig. 4b)**. At 20-kb resolution, we found that pan-sequences were more enriched at
169 TAD boundary regions **(Figs. 4c)**. Notably, we found that genomic variations (SNPs
170 and CNVs) occurred more frequently at TAD boundary regions than at the TAD
171 interior regions **(Supplementary Figs. 10, 11,12 and 13),** indicating that the
172 occurrence of pan-sequences could be associated with genomic variations.

173 Based on the high read coverage of this sample (~300×), we identified 201 (5.4%)
174 pan-sequences which were anchored to genomic regions harbouring putative enhancer

elements. Furthermore, 47 pan-sequences were shown to contain enhancers by demonstrating enhancer-promoter interactions with high confidence **(Supplementary Fig. 14)**. The sequences were significantly enriched in KEGG pathways including retinol metabolism, olfactory transduction, arachidonic acid metabolism and fatty acid degradation **(Supplementary Table 12)**. We also found that some pan-sequences could be divergent alleles in pig genome, resulting in genomic regions of low interaction when only the counterpart of the reference genome is provided. When the corresponding regions of low interaction were replaced with pan-sequences, the 3D spatial structure of the genome was significantly improved **(Fig. 4d)**. Thus, replacement with pan-sequences will help to depict the 3D structures of the whole genome.

Pig pan-genome database

To facilitate the use of the pig pan-genome by the scientific community, a pig pan-genome database (PIGPAN) was constructed. PIGPAN is a comprehensive repository of integrated genomics, transcriptomics and regulatory data. The system diagram is shown in **Fig. 5a**. In our local UCSC Genome Browser server (Gbrowse), 17 tracks were released against the pig pan-genome (**Fig. 5b**). Users can search the database using a gene symbol or chromosome location to obtain results in terms of four aspects: (i) the reference genome and pan-sequence annotations, (ii) the gene expression in 20 corresponding tissues, seven types of regulation signals (**Supplementary Table 13**) and the conserved elements of a 20-way mammalian alignment, (iii) the chromosome localization of pan-sequences, and (iv) the haploid copy number of 87 pigs. We also provided basic search functions to retrieve basic gene information, GO annotation and KEGG pathways. Here, we present one case using PIGPAN showing the copy number difference of KIT between European and Chinese pigs (**Fig. 5c**). Moreover, users can download data from http://animal.nwsuaf.edu.cn/panPig/download.php. As the functions and associated traits of more genes in the pig genome are determined in the future, our browser will be updated regularly to meet the various needs of the scientific community.

Discussion

In this study, we have applied an assembly-versus-assembly approach utilizing twelve independent *de novo* assemblies(Fang, et al. 2012; Li, et al. 2013; Li, et al. 2017) and a large amount of whole-genome resequencing data to build a sequence map of the pig pan-genome. The *de novo* assemblies in the present study cover a wide range of diverse breeds across Eurasia and thus ensure a comprehensive discovery of the missing pan-sequences. These pan-sequences as well as the accompanied genomic variation and expression information will be a valuable resource for depicting the complete genetic makeup of porcine phenotypic and genomic diversity.

With the rapid decrease in the cost of generating high-quality *de novo* assemblies, the pan-genome strategy is becoming increasingly affordable and will soon become applicable for many other animal species. The importance of pan-genomes has been widely accepted in the field of plant genomics(Hirsch, et al. 2014; Schatz, et al. 2014; Golicz, et al. 2016; Gordon, et al. 2017; Sun, et al. 2017; Zhao, et al. 2018). The high genomic plasticity of plants can result in the complete gain/loss of a large number of genes within a species(Golicz, et al. 2016; Gordon, et al. 2017; Zhao, et al. 2018). In contrast, animal genomes are much more conserved and have longer genes with complex splicing events, which means that, generally, only intergenic or fragmented genic regions are involved in the gain/loss of genomic sequences in animals. Nonetheless, this difference does not mean that animal pan-genomes are less important. For instance, the pan-sequences that we recovered demonstrated population-specific patterns, indicating that they are potentially associated with adaptations to various environmental conditions(Li, et al. 2010; Gordon, et al. 2017). Furthermore, our research suggests that these pan-sequences can act as enhancers of some genes that regulate metabolic activity in different breeds. We also found a large number of SNPs residing in the pan-sequences, which can lead to an accurate assessment of true variations, thereby providing enhanced resolution for genetic diversity of different pig populations. The enriched genomic sequence repertoire can help in identifying causal mutations that were previously unrecognized by linkage,

association and copy-number-variation studies.

In conclusion, our study has shown that the pan-genome, when used as a reference, can ensure a more comprehensive repertoire of genomic variations and can facilitate downstream genomic, transcriptomic and even 3D genome analyses(Rao, et al. 2014; Dong, et al. 2017). Therefore, we highlight the transition from the current reference genome to the pan-genome.

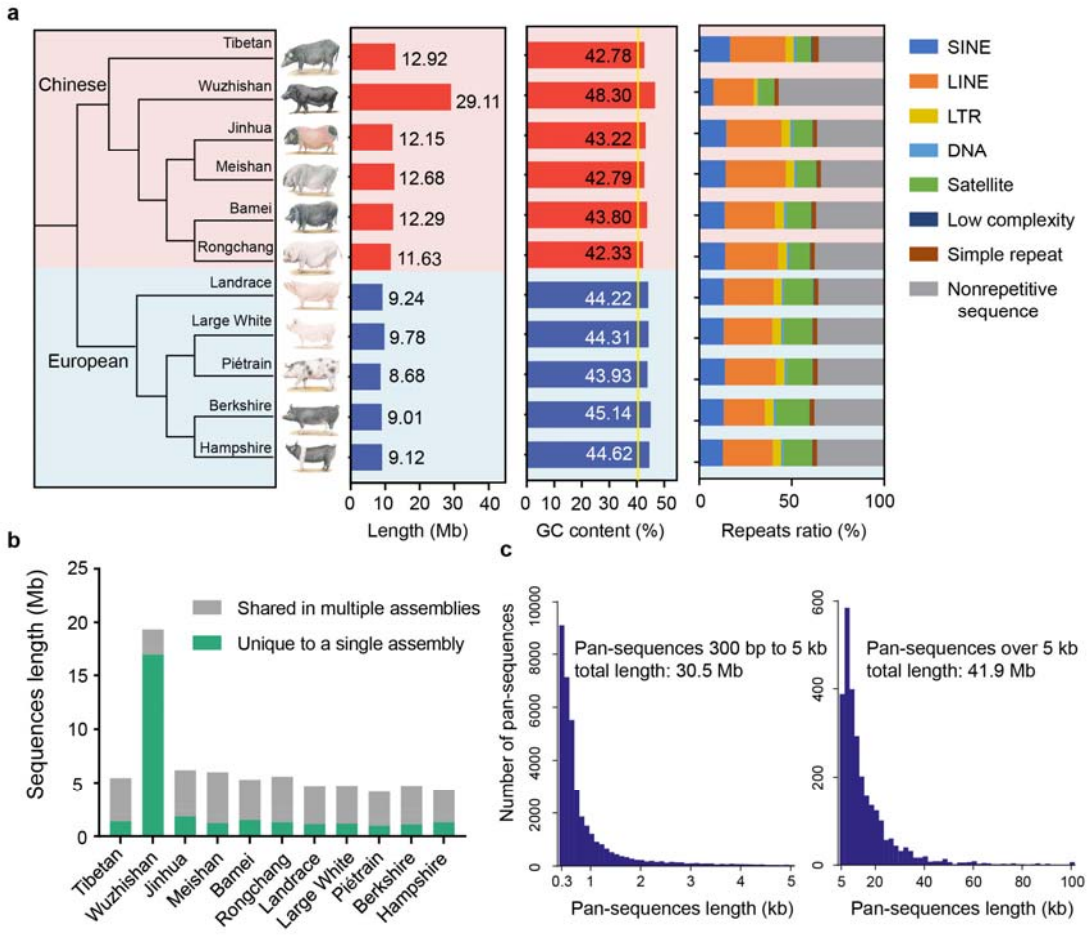

Fig. 1 Construction of the pig pan-genome and the characterization of pan-sequences. a Maximum likelihood phylogenetic tree, sequence length, GC content and repeat composition of missing sequences identified in each individual assembly as compared with Sscrofa11.1. **b** The total sequence length and breed-specific sequence length of each breed for non-redundant pan-sequences. **c** Length distribution of all pan-sequences. (Wuzhishan pigs had the largest number of sequences because this individual is the only male among all the 11 assemblies and the sequencing platform of this individual differed from that used for other samples).

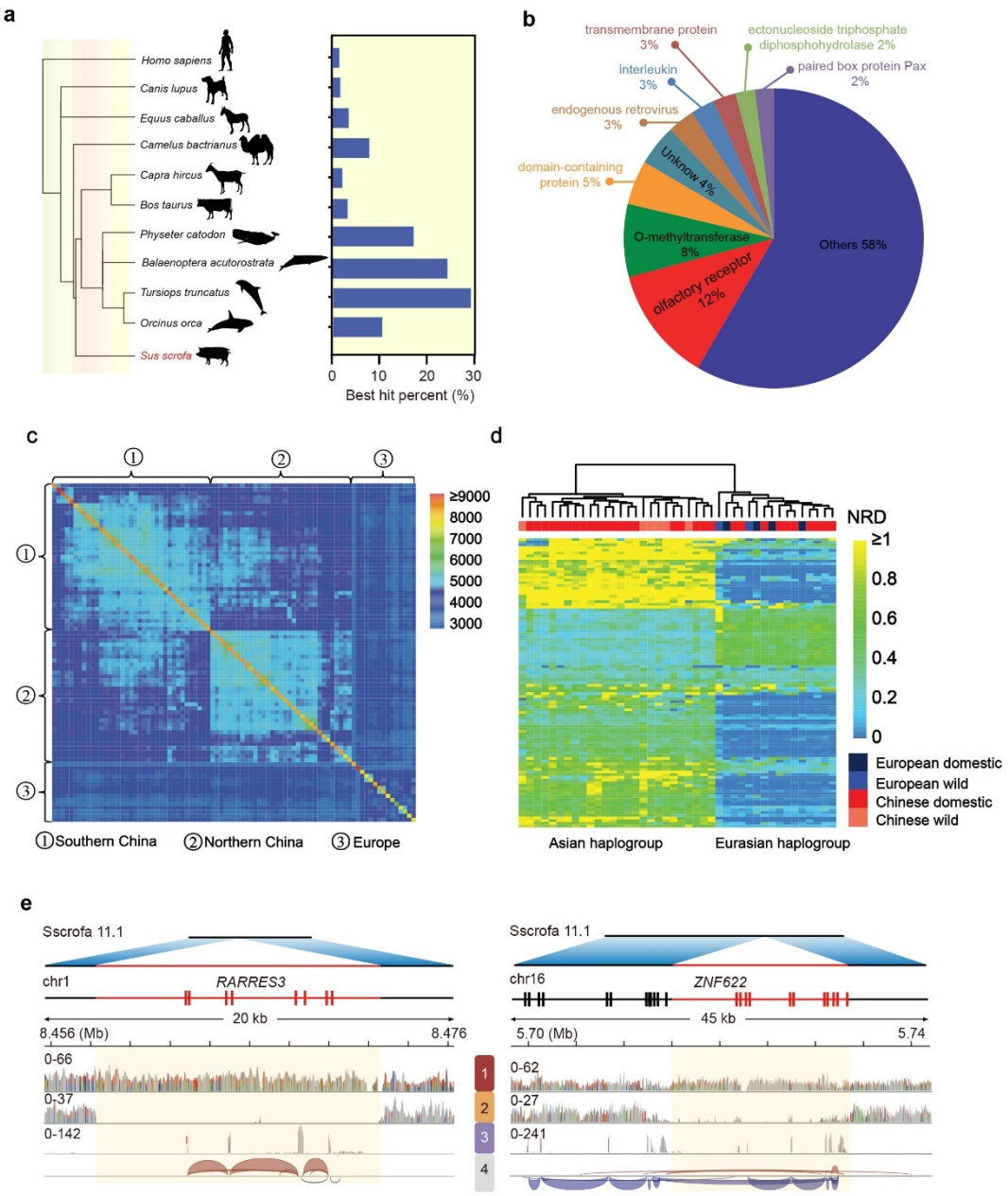

Fig 2. Pan-sequences validation and population-specific pattern. a Homolog identification of pan-sequences in ten mammalian genomes. Only the best hit was retained for each pan-sequence. **b** Number of hits in pan-sequences to Refseq protein families. **c** An 87 × 87 matrix showing the number of shared pan-sequences among all the individuals by pairs. Each cell represents the number of shared pan-sequences by two individuals. See Supplemental table 8 for the classification of each group. **d** The normalized read depth (NRD) of Y chromosome-linked pan-sequences in each male. See Supplemental table 8 for the classification of each group. (Only the sequences with the frequency ranging from 0.5 to 0.9 were shown.) **e** Genes contained in the pan-sequences. One pan-sequence of 14.3 kb harbour

the complete genic region of RARRES3, and another covers partial genic regions of ZNF622, representing a new splicing event. The four tracks at the bottom represent the reads mapping of whole-genome resequencing data of two samples (1-2) and the inferred exons as well as their splicing isoforms based on RNA-seq (3-4).

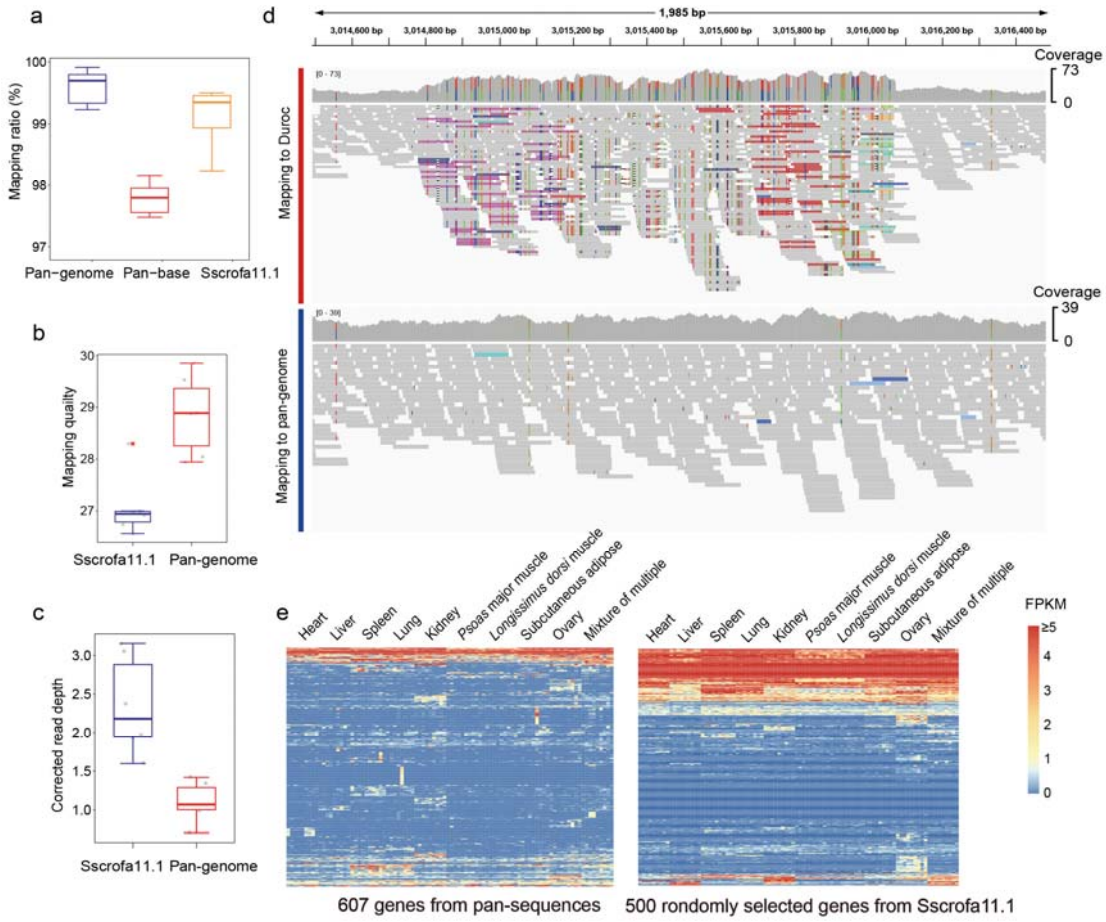

Fig. 3 Improvements of genomic and transcriptomic analyses by using the pan-genome. **a** Comparison of the mapping ratio of resequencing data using the pan-genome versus Sscrofa11.1. **b** Comparison of read-mapping quality using the pan-genome versus Sscrofa11.1. **c** Comparison of corrected read-mapping depth using the pan-genome versus Sscrofa11.1. **d** Improved read mapping using the pan-genome versus Sscrofa11.1 as viewed with IGV. **e** Transcriptional potential of the pan-sequences

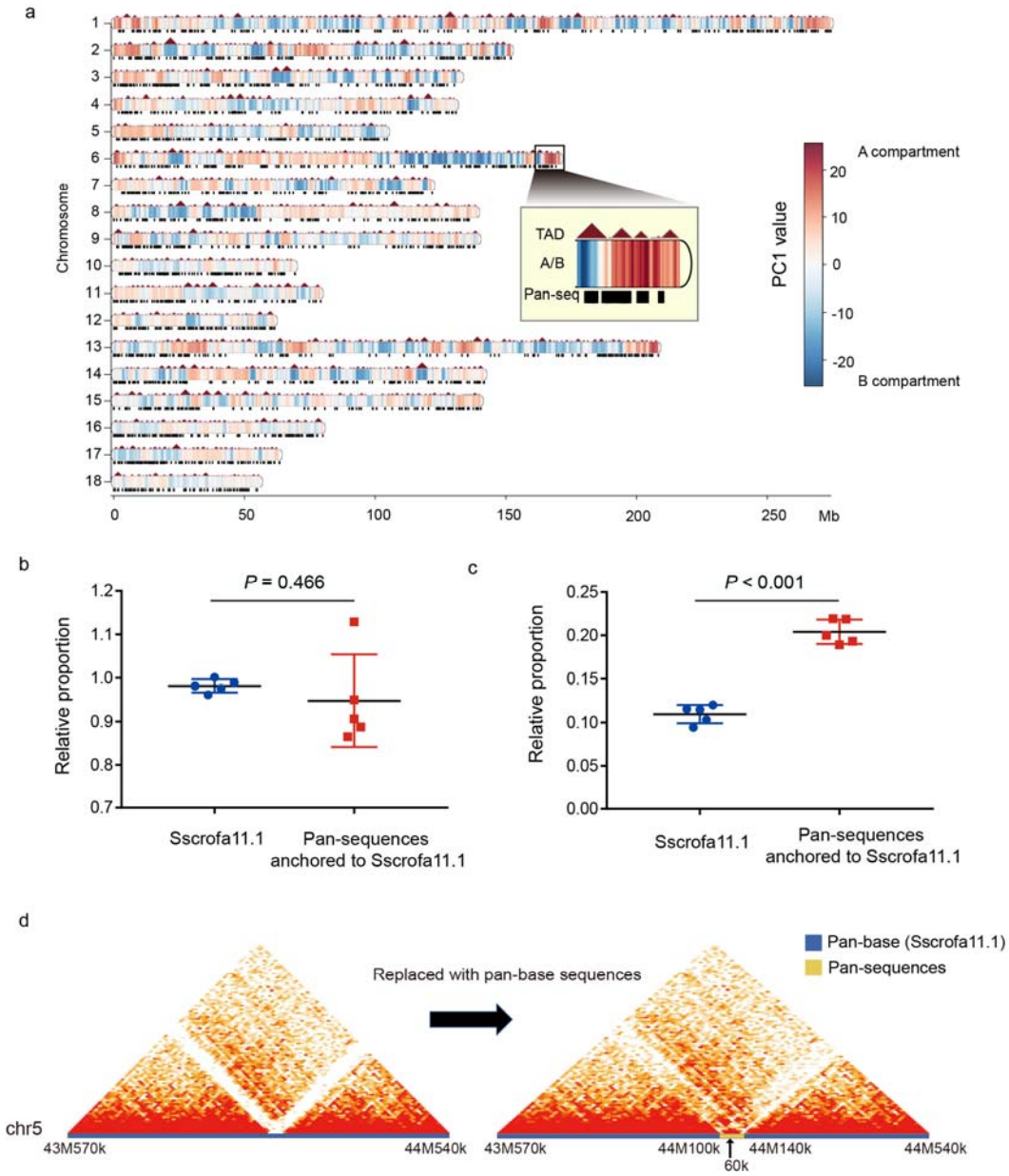

Fig. 4 The 3D spatial structure of the pan-genome. a The distributions of the A/B compartment, TAD and telomere the anchored pan-sequences. **b** The relative proportion of A compartment over B compartment in length in the pig genome (left), and the relative proportion of pan-sequences located in A compartment over those located in B compartment in length (right).**c** The relative proportion of TAD boundary regions over TAD interior regions in length in Sscrofa11.1 (left) and the relative proportion of pan-sequences located in TAD boundary regions over TAD interior regions in length (right). **d** An example of improving a 3D spatial structure after replacing the weakly interacting sequences with the non-reference pan-sequences.

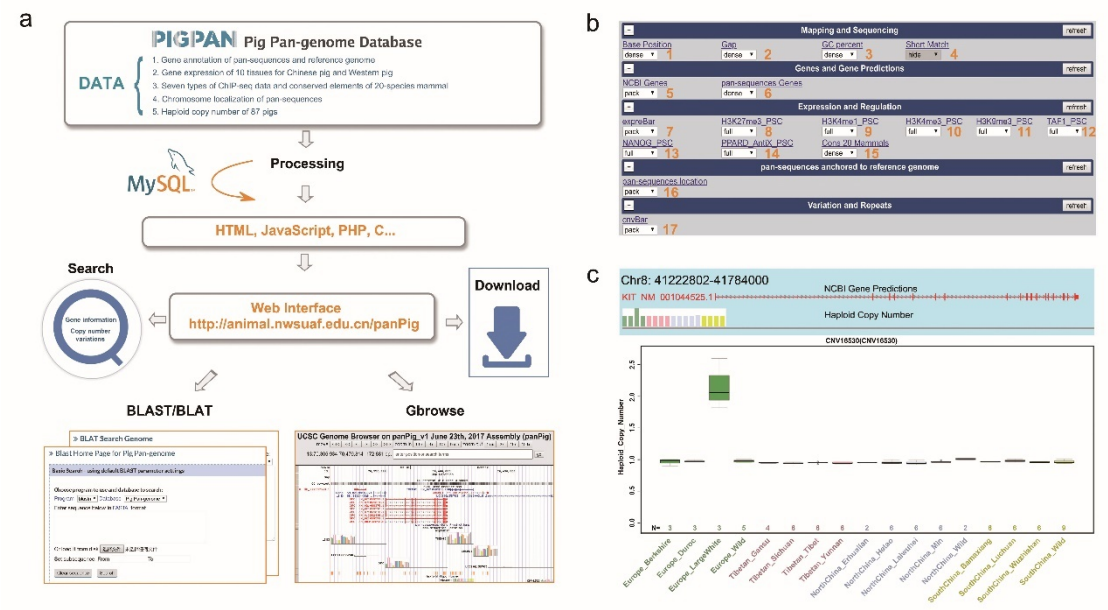

Fig. 5. The processing pipeline used to construct PIGPAN. PIGPAN integrated genomics, transcriptomics and regulatory data. Users can search a gene symbol or a genomic region to obtain results in the form of an interactive table and graph.

Acknowledgements

This work was supported by research grants from the National Natural Science Foundation of China (No. 31572381) to Y.J and the Science & Technology Support Program of Sichuan (2016NYZ0042 and 2017NZDZX0002) to M.Z.L. We thank the High Performance Computing platform of Northwest A&F University for their assistance with the computing.

Author contributions

Y.J. and M.Z. L. conceived the project and designed the research. X.T., Y.L and M.L. analysed the Hi-C data. X.T., R.L., W.F., M.L. and D.D. performed the analysis. X.T., R.L. and W.F. wrote the manuscript. Y.J, M.Z.L., X.W. revised the manuscript.

Competing interests

The authors declare that no competing interests exist.

Methods

Construction of the pan-genome

We downloaded the publicly available pig genome assemblies of ten female and one male individuals from 11 diverse breeds (five originated in Europe and six originated in China) **(Supplementary Fig. 2 and Table 2)**(Fang, et al. 2012; Li, et al. 2013; Li, et al. 2017). To identify the sequences which cannot align to the reference genome, we split the 11 assemblies by gap region and iteratively aligned them to the reference pig genome assembly (Sscrofa11.1) using the BLASTN(Camacho, et al. 2009). Sscrofa11.1 was masked by WindowMasker(Morgulis, et al. 2006) before alignment to speed up the alignment process. The sequences with < 90% identity and ≥ 300 bp in length were retained. After that, these low-identity sequences were aligned to each other to remove redundancy. Finally, a non-redundant set of 72.5 Mb of sequences from 11 assemblies was obtained; these sequences were defined as pan-sequences. The Duroc genome (Sscrofa11.1) plus these 72.5 Mb pan-sequences made up the pan-genome.

Characteristics of the pan-sequences

To explore whether the pan-sequences have homologous regions across species and are potential to be functional, we aligned these sequences to ten mammalian reference genomes (i.e., *Homo sapiens*, *Camelus bactrianus*, *Equus caballus*, *Canis lupus familiaris*, *Capra hircus*, *Bos Taurus*, *Orcinus orca*, *Physeter catodon*, *Balaenoptera acutorostrata scammoni*, *Tursiops truncates*) to search for any matches (*E*-value ≤ 1e-5) using BLASTN(Camacho, et al. 2009)**(Supplementary Table 4)**. Only the best hit was remained for each query.

To validate the authentity of these pan-sequences and identify assembly-specific sequences, we aligned all of them to the each of the 11 *de novo* pig assemblies to search for any matches (⩾90% coverage and ⩾95% identity) using BLASTN(Camacho, et al. 2009). If the sequence of an assembly does not have a high similarity with other assemblies, this sequence is considered as the assembly-specific sequences.

Population-based resequencing and CNV calling

We downloaded the whole genome resequencing data for 71 domestic pigs and 16

326 wild boars for population analysis of pan-sequences. The sequences data were retrived
327 from NCBI under the Bioproject PRJNA213179, PRJNA281548, PRJNA309108 and
328 PRJEB9922(Ai, et al. 2015; Frantz, et al. 2015; Jeong, et al. 2015; Li, et al.
329 2017)**(Supplementary Table5)**. After alignment using BWA (version
330 0.7.15-r1140)(Li and Durbin 2009) with default parameters, we used
331 CNVcaller(Wang, et al. 2017) to calculate the normalized read depth (NRD) of each
332 sequences. The presence and absence of each pan-sequence were then determined by
333 NRD.

334 **ChIP-seq short-read alignment and peak calling**

335 To confirm the content of regulatory elements in pan-sequences, we downloaded
336 seven ChIP-seq data from NCBI Bioproject PRJNA152995, including H3K27me3,
337 H3K4me1, H3K4me3, H3K9me3, NANOG, PPARD AntiX and TAF1 signals **(table**
338 **S13)**(Xiao, et al. 2012). Sequencing reads were aligned to pig pan-genome using
339 BWA (version 0.7.17-r1188)(Li and Durbin 2009) with default parameters.
340 Low-quality and multiple-mapping reads were removed using SAMtools(Li, et al.
341 2009) with option "-q 20". Enriched regions (or peaks) were called ($p < 1e-5$; no
342 filtering on fold enrichment or FDR correction) using MACS (version 2.1.1)(Zhang,
343 et al. 2008) with total DNA input as control.

344 **Male-specific sequences identification**

345 There are 42 males and 45 females in our whole genome resequencing data
346 (Supplementary Table 8). We compared the normalized read depth (NRD) between
347 females (NRD < 0.1, sample size=42) and males (0.2< NRD< 0.7, sample size=45) to
348 identify the putative male-specific pan-sequences. Thus, we identified 1,638
349 male-specific scaffolds (table S9) which were present in most all of male
350 individuals(frequency ⩾ 50%) but absent in females(frequency = 0) with a
351 combined length of 10,432,972bp **(Supplementary Table 6)**.

352 **Gene annotation and functional enrichment analysis**

353 Homology-based and *de novo* prediction were used to annotate protein-coding genes.
354 For homology-based prediction, pan-sequences were aligned onto the repeat-masked

assembly using TblastN(Camacho, et al. 2009) with an *E*-value cutoff of 1e-5. Aligned sequences as well as corresponding query proteins were then filtered and passed to GeneWise to search for accurately spliced alignments(Doerks, et al. 2002). For *de novo* prediction, GenScan(Burge and Karlin 1998), Augustus, and geneid were then used to predict genes.

Annotated genes of novel sequences were analysed for Kyoto Encyclopedia of Genes and Genomes (KEGG) terms and pathway enrichment using KOBAS(Xie, et al. 2011).

SNP calling

To verify whether using the pan-genome as reference could improve SNP calling efficacy, we randomly selected six pig samples (ranging from 10 to 30× coverage) **(Supplementary Table 8)** and mapped their clean reads to the pan-genome and Sscrofa11.1 for comparison. Duplicate reads were removed using Picard Tools. Then, the Genome Analysis Toolkit (GATK, version 3.6)(McKenna, et al. 2010) was used to detect SNPs. The following criteria were applied to all SNPs: (1) Variant confidence/quality by depth (QD) > 2; (2) RMS mapping quality (MQ) > 30.0.

RNA-seq analysis and noncoding RNA prediction

The 92 stand-specific RNA-seq data (7-10 tissue libraries for each of 10 individuals) were downloaded from the NCBI database (Bioproject :PRJNA311523)(Li, et al. 2017). All reads were mapped to the pan-genome by HISAT2(Kim, et al. 2015). Transcripts including novel splice variants were assembled using StringTie version 1.2.2(Pertea, et al. 2015) and the FPKM (Fragments Per Kilobase per Million mapped reads) values for these transcripts and genes in each sample were determined using Ballgown(Frazee, et al. 2015). Finally, transcripts with FPKM ⩾ 1 in at least one sample were retained. After assembling and quantifying all transcripts, the transcripts of pan-sequences were used for identification of high confidence coding RNA by Coding Potential Calculator (CPC)(Kong, et al. 2007) online.

Materials for Hi-C experiment

Liver of BH-33, BH-34, BH-35, and BH-36 were collected from four female

384 2-years-old Bama minipigs. Liver of F2 were collected from a 90-days-old female
385 fetus of Bama minipig. Ear skin fibroblasts DB-2 and DB-3 were established by using
386 two 12-days-old female Large White pigs. Ear skin fibroblasts XYZ were established
387 by using a 2-years-old female Wild Bore. Embryonic fibroblasts RC-7 and RC-8 were
388 established by using two 40-days-old female fetus of Chinese Rong Chang pig.
389 Mature adipocytes DB-2-Y and DB-3-Y were derived from pre-adipocytes which
390 were established by using the same pigs of Ear skin fibroblasts DB-2 and DB-3, by
391 inducing adipogenic differentiation.
392 All of the fibroblasts were grown in DMEM Dulbecco's Modified Eagle Medium
393 (DMEM, 11995-065, Gibco) containing 10% Fetal Bovine Serum (FBS, 10099-141,
394 Gibco) and 1× penicillin/streptomycin (P/S,15140-122, Gibco), incubated at 37℃ in
395 5% CO2.
396 Pre-adipocytes were cultured in 10%FBS/DMEM-F12 (11330-032, Gibco) with
397 1×P/S until confluence and induced to differentiation as previously described. Briefly,
398 two days' post-confluence, cells were exposed to differentiation medium containing
399 0.5 mmol/L isobutylmethylxanthine (I5879, Sigma), 1 μmol/L dexamethasone
400 (D2915, Sigma), 850 nmol/L insulin (I6634, Sigma), 1 μmol/L rosiglitazone (R2408,
401 Sigma) and 10% FBS for three days. At the end of day 3, the differentiation medium
402 was replaced into maintenance medium with only 850 nmol/L insulin, 1 μmol/L
403 rosiglitazone and 10% FBS, and replenished every other day. After the differentiation
404 process, at least 90% of the cells had accumulated lipid droplets at day 15, and were
405 used as mature adipocytes (DB-2-Y and DB-3-Y).
406 **Hi-C experimental method**
407 Hi-C experiment on cells were performed according to the previously published Hi-C
408 protocol with some minor modifications(Lieberman-Aiden, et al. 2009). Briefly, 25
409 million (M) cells were resuspended in 45 ml serum free DMEM, and 37%
410 formaldehyde was added to obtain a final concentration of 2% for chromatin
411 cross-linking. Cells were incubated at room temperature (20−25 °C) for 5 minutes,
412 then glycine was added to obtain a final concentration of 0.25 mol/L to quench the

formaldehyde. The mixture was incubated at room temperature for 5 minutes, and subsequently on ice for at least 15 minutes. Fixed cells were lysed using a Dounce homogenizer in the presence of cold lysis buffer (10 mmol/L Tris-HCl, pH 8.0, 10 mmol/L NaCl, 0.2% IGEPAL CA-630, and 1× protease inhibitor solution). Chromatin digestion (restriction enzyme HindIII), labelling, and ligation steps were performed according to the original protocol(Lieberman-Aiden, et al. 2009). After deproteinization, removal of biotinylated free-ends, and DNA purification, Hi-C libraries were controlled for quality and sequenced on an Illumina Hiseq X Ten sequencer (paired-end sequencing with 150 bp in read length).

Hi-C experiment on liver tissue were performed as previously described using the MboI restriction enzyme(Rao, et al. 2014), with minor modifications pertaining to handling flash frozen primary tissues(Leung, et al. 2015). Briefly, 0.5 g flash frozen liver tissue was pulverized in liquid nitrogen. Then cross-linking by 37% formaldehyde in a final concentration of 4% and incubated at room temperature for 30 mins. Glycine was added to obtain a final concentration of 0.25 mol/L to quench the formaldehyde. The mixture was incubated at room temperature for 5 minutes, and subsequently on ice for at least 15 minutes. Cross-linked liver cells were filtered through 70-μm and 40-μm nylon cell strainers and spinning down to collect the liver cells. About 25 mg liver cell precipitate was used for Hi-C library preparation. The Hi-C library preparation procedure was performed as previously described using the MboI restriction enzyme(Rao, et al. 2014).

Hi-C reads mapping, filtering, and generation of contact matrices

Pre-processing paired-end sequencing data, reads mapping as well as filtering of mapped di-tags was performed using the Juicer pipeline (v.1.8.9)(Durand, et al. 2016). Briefly, short reads were mapped to pan-genome using BWA (version 0.7.15-r1140)(Li and Durbin 2009). Reads of low mapping quality were filtered using Juicer with default parameters, discarding the invalid self-ligated and un-ligated fragments, as well as PCR artefacts. Filtered di-tags were further processed with Juicer command line tools to bin di-tags (10 kb bins) and to normalize matrices with

KR normalization(Knight and Ruiz 2013). Valid Hi-C read pairs should harbor more intrachromosomal (cis) interactions than inter- (trans) **(Supplementary Table 11)**. To improve resolution, we combined the Hi-C data from the same tissue of same pig breed after we randomly extracted 20 Gb data for correlation coefficient test. We combined Hi-C data from DB-2 and DB-3 (Pearson's r = 0.99); RC-7 and RC-8 (Pearson's r = 0.99); DB-2-Y and DB-3-Y (Pearson's r = 0.96). After combined samples, all processes were done in all the data. Normalized interaction matrices were generated at two resolutions of low (100 kb) and high (20 kb) respectively **(Supplementary Figure 15)**.

Identification of compartment A and B

Identification of compartment A/B was performed as previously described using the 100-kb interaction matrix(Lieberman-Aiden, et al. 2009). Principal component analysis (PCA) was performed to generate the first principal component (PC1) vectors of each chromosome, and Spearman's correlation between PC1 and genomic characteristics (gene density and GC content) were then calculated. GC content (%) for each bin (100-kb bin sizes) was calculated using SeqKit (v.0.8.0)(Shen, et al. 2016). Gene density (number of genes per bin) was calculated based on the number of promoters [from -2,000 to +500 bp of transcription start site (TSS)] located in (namely more than 50% of the region should be overlapped) each bin. Compartment A and B were determined by the PC1 values. Bins with positive Spearman's correlation between PC1 values and genomic features were assigned as compartment A, otherwise B.

Identification of topologically associating domains (TADs) and topological boundaries

Higher-resolution TAD calls were generated following the previously described procedure by using the directionality index (DI) metric(Dixon, et al. 2012). DI was calculated using raw interaction counts between 20-kb bins to capture observed upstream or downstream interaction bias of genomic regions. A hidden Markov model (HMM) was then used to predict the states of DI for final TAD generation. The same

criteria 400 kb (distance between two adjacent TADs) was used to distinguish unorganized chromatin from topological boundaries. That is, the topological boundaries are less than 400 kb and unorganized chromatin is larger than 400 kb.

Locating pan-sequences on Sscrofa11.1 based on Hi-C

We normalized all Hi-C matrices on the same scale by KR normalization(Knight and Ruiz 2013), ensuring that any differences between Hi-C are not attributable to variation in sequence length. The maximum 100-kb bin of each pan-sequence interacted (Interaction intensity $\geqslant$ 5) was collected as the potential location of pan-sequences. Starting with the filtered 100-kb resolution bin of pan-sequences, we get the higher resolution interval of 20 kb by taking the maximus 20-kb bin with each 100-kb bin.

Identification of putative promoter and enhancer interactions

We kept the interactions identified by PHYCHIC(Ron, et al. 2017) with FDR < 0.01 as high confidence interactions and used them to identify promoter-enhancer interactions (PEI). Promoter segment was determined as a region from −2,000 to +500 bp of the transcription start site (TSS). When at least half of a promoter segment was in either one of the two bins which involved in a chromatin interaction, this interaction was defined as a putative promoter interaction.

The bins which are distal (at least 40 kb upstream or downstream) from the promoter and demonstrate the strongest interaction with the promoter than other regions were determined as the enhancer interacting with the corresponding promoter. This interaction of the two bins corresponding to the promoter and enhancer was defined as a potential PEI. If our pan-sequences were located on a bin harbouring an enhancer of a PEI, the pan-sequences could be potentially involved in the regulatory functions of the enhancer. If the pan-sequences further demonstrate interactions with the promoter of the same PEI, the involvement of the pan-sequences in the regulatory functions of the enhancer would be regarded as highly confident and the pan-sequences could be a potential enhancer itself.

The pig pan-genome web server

The web interface of PIGPAN was built by combining Apache web server, PHP, HTML, JavaScript and relational database MySQL. Users can use all online resources without preregistration. Our browser can be divided into two parts: frontend and backend interfaces. The frontend consists of a home page, a download page and several search pages. The MySQL relational database server stores 16 tables including gap information, GC percent, seven regulatory signals of potential stem cells (H3K27me3, H3K4me1, H3K4me3, H3K9me3, NANOG, PPARD AntiX, TAF1), conserved elements of 20-species mammal, haploid copy number of 87 pigs, gene expression, location of pan-sequences and gene annotation. The appropriate index was built on the corresponding retrieval columns of the table. When a user submits an entry, the backend will respond quickly to execute an SQL statement. PHP and JavaScript manage the data analysis processes and visualize the results. Moreover, we have introduced web-based software such as BLAST(Camacho, et al. 2009), BLAT(Kent 2002) and Gbrowse(Casper, et al. 2018). Accordingly, users can query data with rapid visualization in Gbrowse or enter a query sequence to search for homologous regions in the genome. PIGPAN was tested in all major modern internet browsers, including Firefox, Chrome, Internet Explorer, Safari and Opera. Therefore, PIGPAN is a robust and easy-to-use website to facilitate the search for and visualization of results for pig pan-genome analyses.

Data availability

The sequencing reads of each sequencing library have been deposited at NCBI for Hi-C data (Project ID: PRJNA496307). The assembly of pig pan-genome and subsequent analysis results are available in our PIGPAN website (http://animal.nwsuaf.edu.cn/code/index.php/panPig). All other data supporting the findings of this study are available in the article and its supplementary Information files or are available from the corresponding author on request.

Ai H, Fang X, Yang B, Huang Z, Chen H, Mao L, Zhang F, Zhang L, Cui L, He W, et al. 2015.

529 Adaptation and possible ancient interspecies introgression in pigs identified by whole-genome
530 sequencing. Nat Genet 47:217-225.
531 Arumemi F, Bayles I, Paul J, Milcarek C. 2013. Shared and discrete interacting partners of
532 ELL1 and ELL2 by yeast two-hybrid assay. Advances in Bioscience and Biotechnology
533 04:774-780.
534 Burge CB, Karlin S. 1998. Finding the genes in genomic DNA. Current Opinion in Structural
535 Biology 8:346-354.
536 Camacho C, Coulouris G, Avagyan V, Ma N, Papadopoulos J, Bealer K, Madden TL. 2009.
537 BLAST+: architecture and applications. BMC Bioinformatics 10:421.
538 Casper J, Zweig AS, Villarreal C, Tyner C, Speir ML, Rosenbloom KR, Raney BJ, Lee CM,
539 Lee BT, Karolchik D, et al. 2018. The UCSC Genome Browser database: 2018 update.
540 Nucleic Acids Res 46:D762-D769.
541 Dixon JR, Selvaraj S, Yue F, Kim A, Li Y, Shen Y, Hu M, Liu JS, Ren B. 2012. Topological
542 domains in mammalian genomes identified by analysis of chromatin interactions. Nature
543 485:376-380.
544 Doerks T, Copley RR, Schultz J, Ponting CP, Bork P. 2002. Systematic identification of novel
545 protein domain families associated with nuclear functions. Genome Res 12:47-56.
546 Dogan ES, Liu C. 2018. Three-dimensional chromatin packing and positioning of plant
547 genomes. Nat Plants 4:521-529.
548 Dong P, Tu X, Chu PY, Lu P, Zhu N, Grierson D, Du B, Li P, Zhong S. 2017. 3D Chromatin
549 Architecture of Large Plant Genomes Determined by Local A/B Compartments. Mol Plant
550 10:1497-1509.
551 Durand NC, Shamim MS, Machol I, Rao SS, Huntley MH, Lander ES, Aiden EL. 2016.
552 Juicer Provides a One-Click System for Analyzing Loop-Resolution Hi-C Experiments. Cell
553 Syst 3:95-98.
554 Fang X, Mou Y, Huang Z, Li Y, Han L, Zhang Y, Feng Y, Chen Y, Jiang X, Zhao W, et al.
555 2012. The sequence and analysis of a Chinese pig genome. Gigascience 1:16.
556 Frantz LA, Schraiber JG, Madsen O, Megens HJ, Cagan A, Bosse M, Paudel Y, Crooijmans
557 RP, Larson G, Groenen MA. 2015. Evidence of long-term gene flow and selection during

558 domestication from analyses of Eurasian wild and domestic pig genomes. Nat Genet
559 47:1141-1148.
560 Frazee AC, Pertea G, Jaffe AE, Langmead B, Salzberg SL, Leek JT. 2015. Ballgown bridges
561 the gap between transcriptome assembly and expression analysis. Nat Biotechnol 33:243-246.
562 Golicz AA, Bayer PE, Barker GC, Edger PP, Kim H, Martinez PA, Chan CK, Severn-Ellis A,
563 McCombie WR, Parkin IA, et al. 2016. The pangenome of an agronomically important crop
564 plant Brassica oleracea. Nat Commun 7:13390.
565 Gordon SP, Contreras-Moreira B, Woods DP, Des Marais DL, Burgess D, Shu S, Stritt C,
566 Roulin AC, Schackwitz W, Tyler L, et al. 2017. Extensive gene content variation in the
567 Brachypodium distachyon pan-genome correlates with population structure. Nat Commun
568 8:2184.
569 Groenen MA, Archibald AL, Uenishi H, Tuggle CK, Takeuchi Y, Rothschild MF,
570 Rogel-Gaillard C, Park C, Milan D, Megens HJ, et al. 2012. Analyses of pig genomes provide
571 insight into porcine demography and evolution. Nature 491:393-398.
572 Guirao-Rico S, Ramirez O, Ojeda A, Amills M, Ramos-Onsins SE. 2018. Porcine
573 Y-chromosome variation is consistent with the occurrence of paternal gene flow from
574 non-Asian to Asian populations. Heredity (Edinb) 120:63-76.
575 Hirsch CN, Foerster JM, Johnson JM, Sekhon RS, Muttoni G, Vaillancourt B, Penagaricano F,
576 Lindquist E, Pedraza MA, Barry K, et al. 2014. Insights into the maize pan-genome and
577 pan-transcriptome. Plant Cell 26:121-135.
578 Jeong H, Song KD, Seo M, Caetano-Anolles K, Kim J, Kwak W, Oh JD, Kim E, Jeong DK,
579 Cho S, et al. 2015. Exploring evidence of positive selection reveals genetic basis of meat
580 quality traits in Berkshire pigs through whole genome sequencing. BMC Genet 16:104.
581 Kent WJ. 2002. BLAT—The BLAST-Like Alignment Tool. Genome Research 12:47-56.
582 Kim D, Langmead B, Salzberg SL. 2015. HISAT: a fast spliced aligner with low memory
583 requirements. Nat Methods 12:357-360.
584 Knight PA, Ruiz D. 2013. A fast algorithm for matrix balancing. Ima Journal of Numerical
585 Analysis 33:1029-1047.
586 Kong L, Zhang Y, Ye ZQ, Liu XQ, Zhao SQ, Wei L, Gao G. 2007. CPC: assess the

587 protein-coding potential of transcripts using sequence features and support vector machine.
588 Nucleic Acids Res 35:W345-349.
589 Larson G, Dobney K, Albarella U, Fang M, Matisoo-Smith E, Robins J, Lowden S, Finlayson
590 H, Brand T, Willerslev E, et al. 2005. Worldwide phylogeography of wild boar reveals
591 multiple centers of pig domestication. Science 307:1618-1621.
592 Leung D, Jung I, Rajagopal N, Schmitt A, Selvaraj S, Lee AY, Yen CA, Lin S, Lin Y, Qiu Y, et
593 al. 2015. Integrative analysis of haplotype-resolved epigenomes across human tissues. Nature
594 518:350-354.
595 Li H, Durbin R. 2009. Fast and accurate short read alignment with Burrows-Wheeler
596 transform. Bioinformatics 25:1754-1760.
597 Li H, Handsaker B, Wysoker A, Fennell T, Ruan J, Homer N, Marth G, Abecasis G, Durbin R,
598 Genome Project Data Processing S. 2009. The Sequence Alignment/Map format and
599 SAMtools. Bioinformatics 25:2078-2079.
600 Li M, Chen L, Tian S, Lin Y, Tang Q, Zhou X, Li D, Yeung CKL, Che T, Jin L, et al. 2017.
601 Comprehensive variation discovery and recovery of missing sequence in the pig genome
602 using multiple de novo assemblies. Genome Res 27:865-874.
603 Li M, Tian S, Jin L, Zhou G, Li Y, Zhang Y, Wang T, Yeung CK, Chen L, Ma J, et al. 2013.
604 Genomic analyses identify distinct patterns of selection in domesticated pigs and Tibetan wild
605 boars. Nat Genet 45:1431-1438.
606 Li R, Li Y, Zheng H, Luo R, Zhu H, Li Q, Qian W, Ren Y, Tian G, Li J, et al. 2010. Building
607 the sequence map of the human pan-genome. Nat Biotechnol 28:57-63.
608 Li YH, Zhou G, Ma J, Jiang W, Jin LG, Zhang Z, Guo Y, Zhang J, Sui Y, Zheng L, et al. 2014.
609 De novo assembly of soybean wild relatives for pan-genome analysis of diversity and
610 agronomic traits. Nat Biotechnol 32:1045-1052.
611 Lieberman-Aiden E, van Berkum NL, Williams L, Imakaev M, Ragoczy T, Telling A, Amit I,
612 Lajoie BR, Sabo PJ, Dorschner MO, et al. 2009. Comprehensive mapping of long-range
613 interactions reveals folding principles of the human genome. Science 326:289-293.
614 Maretty L, Jensen JM, Petersen B, Sibbesen JA, Liu S, Villesen P, Skov L, Belling K, Theil
615 Have C, Izarzugaza JMG, et al. 2017. Sequencing and de novo assembly of 150 genomes

616 from Denmark as a population reference. Nature 548:87-91.
617 McKenna A, Hanna M, Banks E, Sivachenko A, Cibulskis K, Kernytsky A, Garimella K,
618 Altshuler D, Gabriel S, Daly M, et al. 2010. The Genome Analysis Toolkit: a MapReduce
619 framework for analyzing next-generation DNA sequencing data. Genome Res 20:1297-1303.
620 Monat C, Pera B, Ndjiondjop MN, Sow M, Tranchant-Dubreuil C, Bastianelli L, Ghesquiere
621 A, Sabot F. 2017. De Novo Assemblies of Three Oryza glaberrima Accessions Provide First
622 Insights about Pan-Genome of African Rices. Genome Biol Evol 9:1-6.
623 Morgulis A, Gertz EM, Schaffer AA, Agarwala R. 2006. WindowMasker: window-based
624 masker for sequenced genomes. Bioinformatics 22:134-141.
625 Neafsey DE, Waterhouse RM, Abai MR, Aganezov SS, Alekseyev MA, Allen JE, Amon J,
626 Arca B, Arensburger P, Artemov G, et al. 2015. Mosquito genomics. Highly evolvable malaria
627 vectors: the genomes of 16 Anopheles mosquitoes. Science 347:1258522.
628 Nguyen DT, Lee K, Choi H, Choi MK, Le MT, Song N, Kim JH, Seo HG, Oh JW, Lee K, et al.
629 2012. The complete swine olfactory subgenome: expansion of the olfactory gene repertoire in
630 the pig genome. BMC Genomics 13:584.
631 Pertea M, Pertea GM, Antonescu CM, Chang TC, Mendell JT, Salzberg SL. 2015. StringTie
632 enables improved reconstruction of a transcriptome from RNA-seq reads. Nat Biotechnol
633 33:290-295.
634 Rao SS, Huntley MH, Durand NC, Stamenova EK, Bochkov ID, Robinson JT, Sanborn AL,
635 Machol I, Omer AD, Lander ES, et al. 2014. A 3D map of the human genome at kilobase
636 resolution reveals principles of chromatin looping. Cell 159:1665-1680.
637 Ron G, Globerson Y, Moran D, Kaplan T. 2017. Promoter-enhancer interactions identified
638 from Hi-C data using probabilistic models and hierarchical topological domains. Nat
639 Commun 8:2237.
640 Schatz MC, Maron LG, Stein JC, Wences AH, Gurtowski J, Biggers E, Lee H, Kramer M,
641 Antoniou E, Ghiban E, et al. 2014. Whole genome de novo assemblies of three divergent
642 strains of rice, Oryza sativa, document novel gene space of aus and indica. Genome Biology
643 15.
644 Shen W, Le S, Li Y, Hu F. 2016. SeqKit: A Cross-Platform and Ultrafast Toolkit for FASTA/Q

645 File Manipulation. PLoS One 11:e0163962.
646 Shyu RY, Jiang SY, Chou JM, Shih YL, Lee MS, Yu JC, Chao PC, Hsu YJ, Jao SW. 2003.
647 RARRES3 expression positively correlated to tumour differentiation in tissues of colorectal
648 adenocarcinoma. Br J Cancer 89:146-151.
649 Sun C, Hu Z, Zheng T, Lu K, Zhao Y, Wang W, Shi J, Wang C, Lu J, Zhang D, et al. 2017.
650 RPAN: rice pan-genome browser for approximately 3000 rice genomes. Nucleic Acids Res
651 45:597-605.
652 Tang Q, Gu Y, Zhou X, Jin L, Guan J, Liu R, Li J, Long K, Tian S, Che T, et al. 2017.
653 Comparative transcriptomics of 5 high-altitude vertebrates and their low-altitude relatives.
654 Gigascience 6:1-9.
655 Wang X, Zheng Z, Cai Y, Chen T, Li C, Fu W, Jiang Y. 2017. CNVcaller: highly efficient and
656 widely applicable software for detecting copy number variations in large populations.
657 Gigascience 6:1-12.
658 Wong KHY, Levy-Sakin M, Kwok PY. 2018. De novo human genome assemblies reveal
659 spectrum of alternative haplotypes in diverse populations. Nat Commun 9:3040.
660 Xiao S, Xie D, Cao X, Yu P, Xing X, Chen CC, Musselman M, Xie M, West FD, Lewin HA,
661 et al. 2012. Comparative epigenomic annotation of regulatory DNA. Cell 149:1381-1392.
662 Xie C, Mao X, Huang J, Ding Y, Wu J, Dong S, Kong L, Gao G, Li CY, Wei L. 2011. KOBAS
663 2.0: a web server for annotation and identification of enriched pathways and diseases. Nucleic
664 Acids Res 39:W316-322.
665 Yan G, Zhang G, Fang X, Zhang Y, Li C, Ling F, Cooper DN, Li Q, Li Y, van Gool AJ, et al.
666 2011. Genome sequencing and comparison of two nonhuman primate animal models, the
667 cynomolgus and Chinese rhesus macaques. Nat Biotechnol 29:1019-1023.
668 Zhang X, Firestein S. 2002. The olfactory receptor gene superfamily of the mouse. Nat
669 Neurosci 5:124-133.
670 Zhang Y, Liu T, Meyer CA, Eeckhoute J, Johnson DS, Bernstein BE, Nusbaum C, Myers RM,
671 Brown M, Li W, et al. 2008. Model-based analysis of ChIP-Seq (MACS). Genome Biol
672 9:R137.
673 Zhao Q, Feng Q, Lu H, Li Y, Wang A, Tian Q, Zhan Q, Lu Y, Zhang L, Huang T, et al. 2018.

674 Pan-genome analysis highlights the extent of genomic variation in cultivated and wild rice.
675 Nat Genet 50:278-284.
676